Fast response of global monsoon area and precipitation to regional carbonaceous aerosols

A Asutosh[1,2*], V. Vinoj[1], K. Landu[1] & H. Wang[3]

[1]School of Earth, Ocean and Climate Sciences

Indian Institute of Technology Bhubaneswar, Bhubaneswar, Odisha, INDIA 752 050

[2]National Center for Atmospheric Research, Boulder, CO, USA

[3]Atmospheric and Global Changes Division, Pacific Northwest National Laboratory, Richland, WA, USA – 99352

*Correspondence: asutosh.acharya@gmail.com

Abstract

Monsoon exerts a significant social and economic impact on billions of people around the world. Changes in global monsoon (GM) rainfall under global warming have been well studied; however, the understanding of GM connection with regional aerosol emissions is limited. Using an atmospheric general circulation model (AGCM), we attempt to quantify the response of global monsoon area and precipitation the removal of carbonaceous aerosols over North America (AM), North Africa (AF), Europe (EU), and Asia (AS). The global average aerosol optical depths (AOD) are reduced by 2.21%, 1.8%, 1.16 %, and 3.8% respectively. A southward shift in the GM domain is observed, responding to changes in magnitude and position of the Inter-Tropical Convergence Zone, when carbonaceous aerosols are removed over these regions in the Northern Hemisphere. The percentage departure in the area-averaged GM precipitation is found to be 4-fold in magnitude for the removal of emissions in EU when compared to that of AM and AF. A shrinkage in the GM area is also observed, which is in maximum for EU (~ - 30 %) compared to AM and AF (~ -25%). The response of GM precipitation and area is found to be the least and opposite in nature for AS emissions. This study provides insight into the regional nature of carbonaceous aerosol effects on global precipitation.

Keywords: Global monsoon, carbonaceous aerosols, aerosol optical depth, GCM, fast response

1. Introduction

Monsoon is generally characterized by a seasonal reversal of lower tropospheric winds as a response to large-scale land-sea thermal contrast (Webster et al., 1998) and north-south movement of the intertropical convergence zone (ITCZ). Monsoon rain has a large socioeconomic impact on two-thirds of the world's population (Hsu et al., 2012; Kitoh et al., 2013). It is essential for infrastructure planning, food security, ecosystem services, and sustainable economic development (Liu et al., 2016a). Understanding the change in monsoon rainfall is of great scientific and societal interest. Investigating how monsoon precipitation has changed in the historical period may provide insight into understanding future monsoon changes (Wang, 2006). Each regional monsoon has distinct characteristics in terms of variability (Kripalani and Kulkarni, 2001; Meehl et al., 2007; Schreck and Semazzi, 2004; Turner and Annamalai, 2012; Yu et al., 2004). These regional monsoon variabilities often result from variations in land surface alignment and characteristics concerning the adjacent oceans and global teleconnections (Li et al., 2016a; Wang and Ding, 2006). Hence, a global perspective of monsoon study is desirable to be investigated changes as a whole (Zhou et al., 2008) considering the physical principle of conservation of mass, moisture, and energy as it applies to the global atmosphere and its exchange of energy with the underlying surfaces (Trenberth et al., 2000; Wang and Ding, 2006)

Understanding the global monsoon (GM) involves studying all aspects of the physical climate system (i.e., atmosphere, ocean, land, and cryosphere), including the role of human-made influences. Changes in GM appear in rainfall intensity and the spatial extent or area covered by monsoon rain (Hsu et al., 2012). Studies from historical precipitation records show that global land monsoon has a decreasing trend during the second half of the 20th century (Ramesh and Goswami, 2007; Wang and Ding, 2006). On the other hand, the combined monsoon

precipitation (over land and ocean) has shown an increasing trend during recent years (Hsu et al., 2011; Wang et al., 2012). Modeling studies using CMIP5 simulations have revealed that the GM precipitation and area will potentially be enhanced in future warming scenarios (Kitoh et al., 2013; Lee and Wang, 2014).

Anthropogenic aerosols are one of the major factors contributing to human-induced climate change, particularly in densely populated regions like Asia (Gao et al., 2022; Li et al., 2016b; Ramanathan et al., 2005a; Sanap and Pandithurai, 2015). Anthropogenic aerosols partly offset greenhouse warming (Li et al., 2016b; Samset et al., 2018). Due to its spatially inhomogeneous nature, aerosol can alter regional rainfall, evaporation, boundary layer process, and circulation(Lau, 2016; Rotstayn et al., 2007). The spatial inhomogeneity of aerosol forcing further results in increased and compensating convections far away from aerosol sources (Liu et al., 2023; Menon, 2002; Rotstayn et al., 2007; Xie et al., 2020). Also, a few studies show that regional (Guo and Yin, 2015; Shawki and Voulgarakis, 2018; Vinoj et al., 2014) and global rainfall (Iles and Hegerl, 2014; Liu et al., 2016a) can be greatly impacted by remote aerosols. For example, based on a modeling study, Liu at al. (Liu et al., 2016b) found that the northern hemispheric (NH) volcanic eruptions are more efficient in reducing the NH monsoon precipitation than the equatorial ones, and so do the southern hemispheric (SH) eruptions in weakening the SH monsoon. In another modeling study, it was found that Australian rainfall was impacted by Asian aerosols (Rotstayn et al., 2007). Recently using the Precipitation Driver Response Model Intercomparison Project (PDRMIP) simulations, Xie et al.(Xie et al., 2020) found that both Asian and Global carbonaceous aerosols can have a significant potential to modulate the Asian monsoon system. A few more studies highlight the impacts of remote aerosol on the Asian/Indian monsoon (Bollasina et al., 2014; Chakraborty et al., 2013; Guo et al., 2016).

Although the role of greenhouse warming in modulating global monsoon is well known (Cherchi et al., 2011), the impact of aerosols on GM variabilities are yet to be investigated in detail (Liu et al., 2016a; Wang et al., 2013). Understanding the climate impacts of carbonaceous aerosols is extremely important among the different aerosol species at a regional and global scale. Mostly, the black carbon (BC) component of carbonaceous aerosols can absorb radiation and have large positive radiative forcing (Stocker et al., 2013), but could also lead to solar dimming (Ramanathan et al., 2005b) and hence is known to reduce precipitation locally. BC has significant impacts on climate and hydrological cycle(Ganguly et al., 2012; Lau et al., 2006; Lou et al., 2019; Sanap and Pandithurai, 2015; Yang et al., 2019; Zhou et al., 2020). Numerous studies have shown the effect of carbonaceous aerosols on the Asian monsoon system (Lau, 2016; Meehl et al., 2008; Sanap et al., 2014). However, these studies are mostly confined to regional rainfall changes. Except for a few studies (Ha et al., 2020; Liu et al., 2016a; Man et al., 2021), a comprehensive understanding of aerosols (especially carbonaceous aerosols) induced changes to GM is still lacking.

This paper attempts to characterize the possible response of GM precipitation and area to spatially varying carbonaceous aerosols. We have further tried to quantify the relative changes in global monsoon characteristics with respect to forcing asymmetry from individual carbonaceous aerosol emission hotspots.

It is to be noted that this study primarily intends to investigate the fast climate response (Bala et al., 2010a; Hansen, 2005) of GM precipitation to regionally varying carbonaceous aerosols. Hence the experiments were designed using prescribed sea surface temperature (Hansen, 2005). It is essential to mention that GM can also be altered through the aerosol-induced slow

response through the ocean pathway; however, it is beyond the scope of the present study and will be investigated in the future.

The rest of this paper is structured as follows. Section 2 provides a brief description of the model used, numerical experiments, and methodology of the study, as well as the definition of global monsoon. Section 3 explains the evaluation of global monsoon and presents the results from numerical experiments along with a proposed physical mechanism for monsoon responses, followed by a discussion and conclusion in section 4.

2. Data and Methodology

The Community Atmosphere Model version 5 (CAM5) is used to investigate the response of global monsoon precipitation to carbonaceous aerosols. The model is developed at the National Center for Atmospheric Research (NCAR), with some modifications in aerosol removal and convective transport (Wang et al., 2013). CAM5 has substantial enhancements to representing the atmospheric processes compared to its earlier versions. Also, the model has a detailed representation of the aerosol lifecycle, which enables the model to be used for investigating aerosol-climate interactions. It includes aerosol species such as primary organic matter (POM), BC, secondary organic aerosol, mineral dust, sulfate, and sea salt, each of which experiences the full aerosol lifecycle of coagulation/condensation growth, transport, interactions with clouds, wet and dry deposition (Liu et al., 2012; Ma et al., 2013). CAM5 also has a physics diagnostic package for studying the direct, semi-direct, and indirect effects of aerosols (Ghan et al., 2012). The CAM5 aerosol model uses a modal aerosol treatment of three size modes (Aitken, accumulation, and coarse mode) (Kay et al., 2015; Liu et al., 2012). Species mass mixing ratios, as well as a number concentration, are predicted for each mode. For the present work, the aerosol emission datasets are the same as the ones used for the

Intergovernmental Panel on Climate Change (IPCC) Assessment Report (AR5) model inter-comparison activities (Lamarque et al., 2010). The emission inventory for the year 2000 represents the combination of existing global and regional inventories, a total of 12 sectors are used to represent various emission sources of gases and aerosol distribution. Using this dataset, the AOD and simulated aerosol diagnostics are in good agreement with the results documented in previous research.

The rapid radiative transfer method for general circulation models (RRTMG) provides radiative transfer calculations. More details of the model can be found in some previous studies (Liu et al., 2012; Wang et al., 2013). The model configuration used for this study is provided in Supplementary Table 1.

2.1 Experimental Setup

The present study focuses on the response of global monsoon rainfall to northern hemispheric (NH) carbonaceous aerosols. Therefore, we have perturbed carbonaceous aerosols over spatially separated aerosol hotspots such as Northern America (AM), Western Europe (EU), North Africa (AF), and Asia (AS), as marked by boxes in Fig.1.

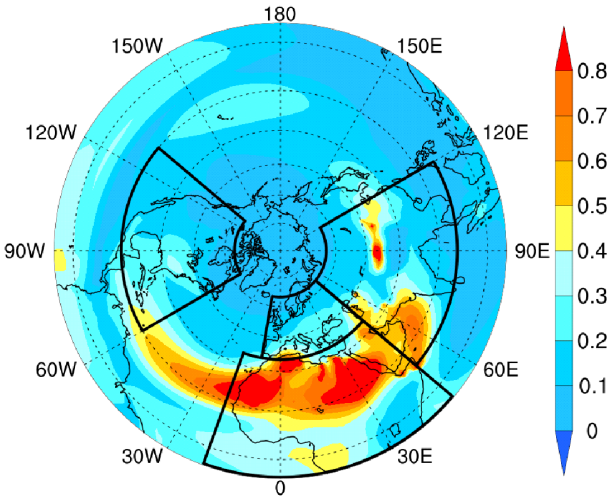

Figure 1. Mean annual aerosol optical depth (CTRL) over the northern hemisphere with the boxes marking the regions where carbonaceous aerosols are perturbed

In addition to the control simulation (CTRL) with all aerosol species included, we perturbed carbonaceous aerosols over the different regions marked by boxes in Figure 1. Each of these simulations was carried out for 10 years (equilibrium runs). A total of five simulations were conducted and summarized in Table 1.

Table 1: Simulations performed for this present study

Simulations	Name	Remark/Details
Control	CTRL	With all aerosol types
Experiment 1	AM	All aerosols except carbonaceous aerosols (POM, BC) over North America (AM)
Experiment 2	AF	All aerosols except carbonaceous aerosols (POM, BC) over North Africa (AF)
Experiment 3	EU	All aerosols except carbonaceous aerosols (POM, BC) over Europe (EU)
Experiment 4	AS	All aerosols except carbonaceous aerosols (POM, BC) over Asia (AS)

2.2 Observational Datasets

The GM analysis in the past generally used the Global Precipitation Climatology Project (GPCP) and CPC Merged Analysis of Precipitation (CMAP) widely (Wang and Ding, 2008; Zhou et al., 2008). However, a comparison of these two datasets suggested the use of GPCP over CMAP precipitation data due to its higher reliability (Hsu et al., 2011). GPCP covers both land and ocean and combines rain gauge data and satellite estimates.

We use GPCP version 2.2, monthly combined datasets to characterize the global monsoon domain and evaluate model simulations. The datasets are recorded by the World Climate Research Program (WCRP) (Adler et al., 2003) with a horizontal resolution of 2.5º. For this study, we use 20 years of data from the year 1991-2010.

2.3 Global monsoon definition

The global monsoon precipitation domain is delineated based on the contrast between rainy summer and dry winter (Wang and Ding, 2006). This contrast is an essential characteristic of the monsoon climate (Webster et al., 1998). Global monsoon consists of regional monsoon regions, including the North American monsoon (NAM), North African monsoon (NAF), Indian monsoon (IND), East Asian monsoon (EAS), Western North Pacific monsoon (WNP), South American monsoon (SAM), South African monsoon (SAF), and the Australian monsoon (AUS). The global monsoon domain (GMD) is also defined by the yearly range of precipitation (Wang and Ding, 2008). The annual range (AR) of monsoon precipitation is the difference between local summer and winter precipitation hence providing the fundamental parameter in defining the monsoon precipitation region (Lee et al., 2013; Wang et al., 2012). Other previous studies defined the GMD with slightly different definitions (Lee et al., 2013). Regardless of the difference, the sign of the calculated GM precipitation trends is the same (Hsu et al., 2011). In this study, GMD is defined based on two criteria (Liu et al., 2009). The AR needs to exceed 2 mm day^{-1}, and the local summer rainfall exceeds 55% of the annual total rainfall. It is interesting to note that the global monsoon region is primarily controlled by local summer rainfall and is not sensitive to local summer to the annual rainfall ratio (Hsu et al., 2012). This is because the maximum fraction of annual rainfall at a location comes from the summer rain.

We have further calculated the total GM precipitation within the control experiment GMD but in the emission perturbation experiments to see if there is any change in climatological mean precipitation due to emission perturbations. Further, the total area of GMD is calculated for each of the five experiments and defined as global monsoon area (GMA)

3. Results

3.1 Changes in aerosol optical depth

Aerosol optical depth (AOD) is the column measure of solar light attenuation by aerosols. It also serves as a quantitative estimate of the amount of aerosol present in the atmosphere. Figure 2 depicts the percentage change in AOD due to the removal of carbonaceous aerosols emissions over the regions marked in Figure 1. The percentage decline in AOD is more than 30% due to the emissions over the AM and AS regions. Though emissions of carbonaceous aerosols are removed locally, the effects are pronounced throughout the globe. Due to the emission removal, the net decline in global average AOD is -2.21%, -1.8%, -1.16 %, and -3.8% for AM, AF, EU, and AS emission reductions respectively. Global anthropogenic aerosol emission hotspots are mostly present in the northern hemisphere, and hence the AOD percentage changes due to emission removal are at a maximum in the northern hemisphere.

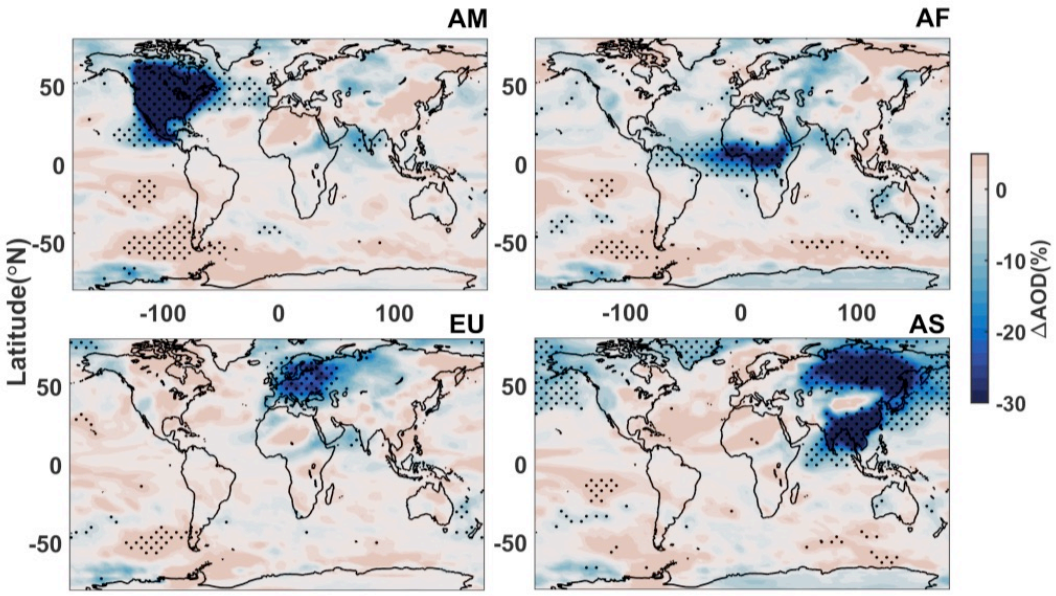

Figure 2. Annual percentage change in spatial aerosol optical depth as a response to the removal of carbonaceous aerosol emissions. Stipples show areas being significant at 95% confidence level, obtained using a student t-test for the mean difference

Among the four emission removal regions, the maximum decline in northern hemispheric AOD is due to removal of AS carbonaceous aerosol emission (-7.3 %), followed by AM (-5.2 %). The African and European emission removal result in near similar magnitude in AOD changes (-2.64 % and -2.60 %, respectively), when averaged over the northern hemisphere. Interestingly, the removal of AS emissions leads to a significant change in AOD over Greenland, the northeastern pacific, and even distant places like Australia in the southern hemisphere, which is consistent with the far-reaching impact of Asian emissions on global aerosols based on aerosol source tagging studies (Yang et al., 2017). Similarly, the effects of African and American emissions are seen far away from the source regions (over the Arabian Sea, Bay of Bengal, Australia, and parts of the Pacific, Atlantic, and Southern Ocean, etc.,) with an increase or decrease in AOD. These regions are most important to global monsoon dynamical and physical processes. Such redistributions in AOD and other aerosol properties may change the aerosol radiative forcing regionally which might further impact the hydrological cycle as reported in earlier studies (Guo and Yin, 2015; Myhre et al., 2017; Xie et al., 2020). Please note that these remote effects of regional changes in aerosols could be due to the response of various forcing and feedback and may not necessarily be the transport of these aerosols elsewhere (Xie et al., 2020).

220 **3.2 Simulation of global monsoon domain and precipitation**

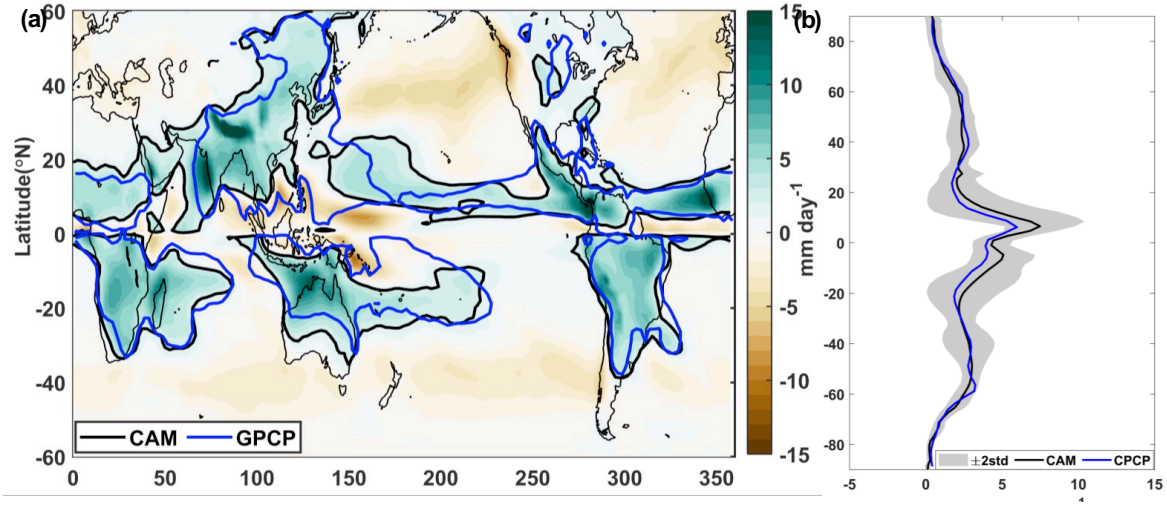

221

222 **Figure 3.** (a) Characterizations of the global monsoon domain in CAM5 (black) and GPCP
223 (blue). Shading shows the Annual Range (AR) of CAM5, (b) the annual zonal averaged
224 precipitation, and the shading shows 95% confidence Intervals (±2 standard deviations of
225 CAM5 CTRL simulation

226 Figure 3a shows the global monsoon domains in CAM5 (black line) and GPCP (blue line),
227 respectively, calculated using the methodology explained in section 3.3. The shading shows
228 the annual range (AR) of precipitation (local summer minus winter months both in NH and
229 SH) for the CAM5 CTRL experiment. The patterns are matching well between the model and
230 GPCP. However, a minor difference arises due to the different grid sizes between the model
231 and observation. Additionally, all continental monsoon regions have a large annual range of
232 precipitation in comparison with their annual mean values.

233 Figure (3b) in the right panel depicts the zonal averaged latitudinal variation of annual
234 precipitation for CTRL (CAM) and GPCP. The shading shows ±2 standard deviations of the
235 CTRL simulation. The latitudinal variation in rainfall for both CTRL and GPCP also shows a
236 good agreement with each other.

3.3 Changes in the global monsoon domain due to aerosol perturbations

To understand the impact of removal of regional carbonaceous aerosol emissions on the global monsoon, we show in Fig. 4 a comparison of the GMD between the CTRL and the perturbation experiments (described in Table 1).

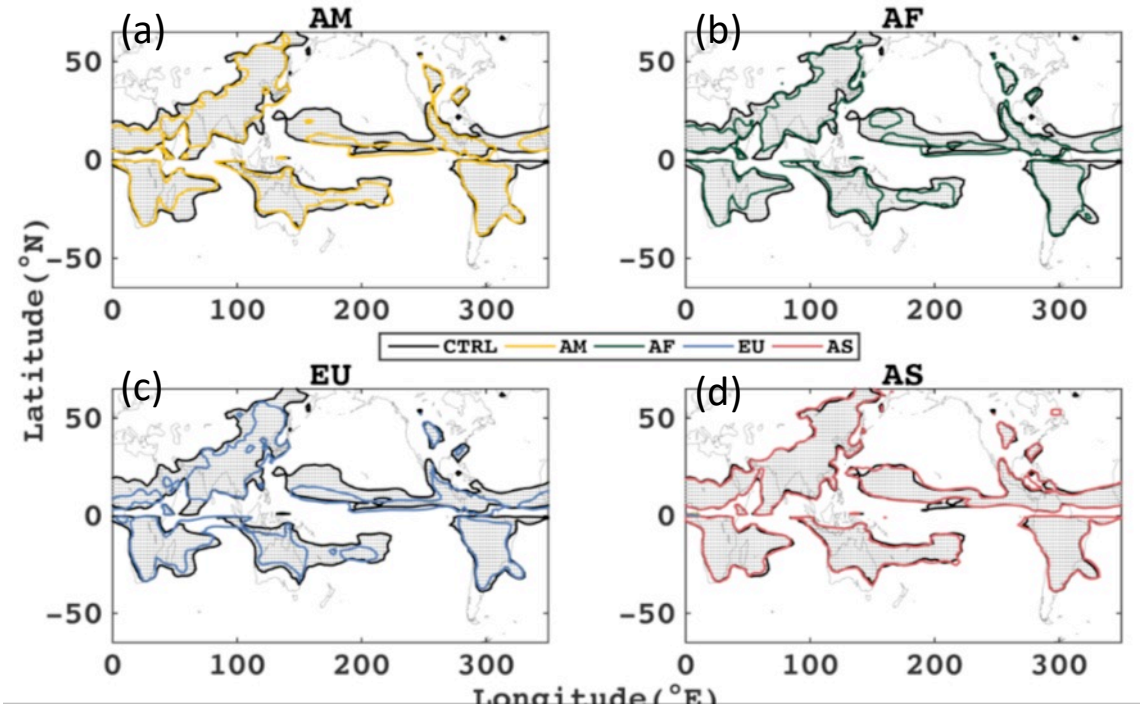

Figure 4. Simulation of global monsoon domain in CTRL (black) and individual emission perturbation experiments. The black line with grey shading shows the extent of the global monsoon for the CTRL. Different colors have been assigned for the monsoon domain corresponding to perturbation experiments.

In Fig. 4, the results show a significant and distinct change in the GMD response to all the emission perturbations (except AS). The removal of North American emissions expands the global monsoon domain further south over the Pacific Ocean along with maximum changes (shrinkage) over South Africa (Figure 4a).

The monsoon domain shrinks over African regions when the emissions of carbonaceous aerosols are removed over North Africa. Also, it splits the Australian monsoon domain into

two parts. On the other hand, the monsoon regions in the northern hemisphere are mostly affected by the perturbation of European aerosol emissions with a maximum reduction over North Africa and Asian monsoon regions. Additionally, similar to that of AF, it has a far-reaching impact on the Australian monsoon domain. It is interesting to note that the Asian aerosol emission removal has the least impact locally/regionally compared to the other emission perturbations, although it reduces the overall GM domain.

3.4 Changes in the global monsoon area (GMA)

To quantify the response of the global monsoon to the removal of each of these aerosol hotspots, we calculated the area of global monsoon domain for the CTRL and each of the perturbation experiments.

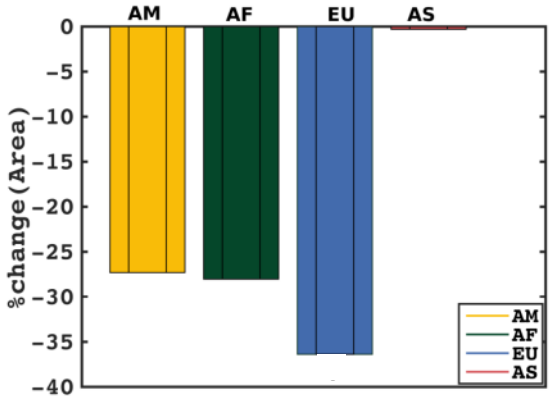

Figure 5. Percentage change in GM areas in all four perturbation experiments with respect to CTRL.

Figure 5 depicts the percentage change in the area/spread of GMD for separate perturbation experiments relative to CTRL. Irrespective of the source, the removal of emissions if carbonaceous aerosols lead to a contraction in GMA. The maximum reduction in the area is observed for the removal of European carbonaceous aerosol emissions (> 35 %). The African and American perturbations have a similar response to GMD area changes (~25 %). However, the perturbation of Asian aerosol emissions is found to be the least among all.

3.5 Changes in global monsoon precipitation

It is interesting to further investigate how GM precipitation responds to the carbonaceous aerosol emissions removals from region-specific northern hemispheric pollution hotspots. Figure 6a shows the percentage change in precipitation within the control GMD. We have calculated the average precipitation rates for each perturbation experiment within the GMD of CTRL.

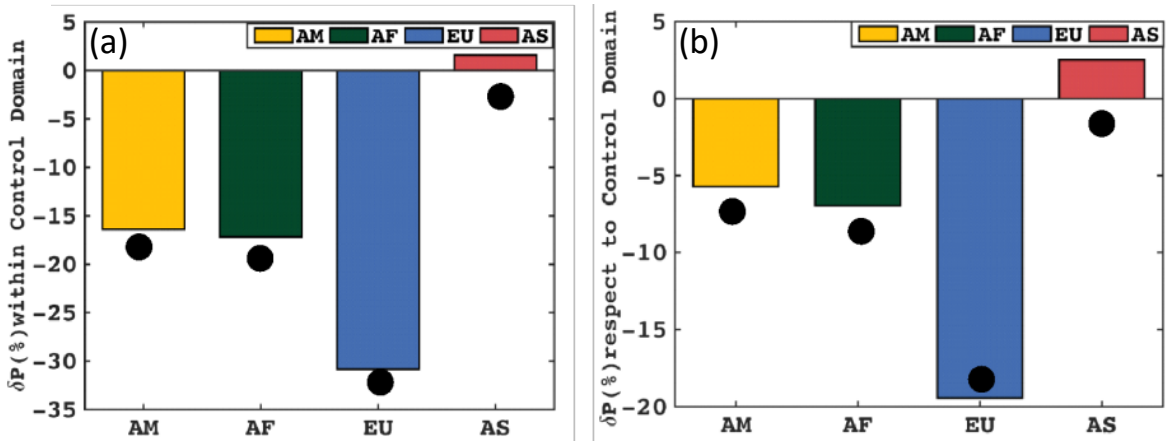

Figure 6. (a) Percentage change in global monsoon precipitation within the control domain for all the perturbation experiments and (b) Percentage change in precipitation of corresponding domains relative to the control domain. The black dots represent the result which is significant ($p <= 0.05$) for the mean difference over all the grid boxes obtained using the student's t-test.

Once carbonaceous aerosols emissions are removed, there is a significant reduction ($p< 0.05$) in precipitation found within the control GM domain for each perturbation experiment. Likewise, in response to the GM area, the European carbonaceous aerosols show the maximum negative impact on the precipitation within the control GMD and are responsible for around ~30% reduction in precipitation. Interestingly, the response to the removal of American and African carbonaceous aerosol emissions is nearly similar (~15%). Though the net GM area shrinks a little due to the removal of Asian emissions, there is a slight increase in rainfall within the control domain. These results suggest nonlinear aerosol-global monsoon relationships, which largely depend on the spatiotemporal change in aerosols and the

associated feedback (Shawki et al., 2018; Xie et al., 2020). As shown in Figure 4, there is a shift in the GMD, and the corresponding spreads are different for each of the perturbation experiments. We have further calculated the percentage change in precipitation between individual global monsoon domains (color contours in Figure 4) corresponding to the control domain (solid black contour in Figure 4), represented in Figure 6b. It is important to note that there is a net decline in the area-averaged precipitation due to the removal of carbonaceous aerosol emissions when compared to the control simulation. The net change is negative for all three aerosol emissions regions except Asia. Near 20 % decline in the total precipitation rate is observed when European carbonaceous aerosol emissions are removed from the model. In the case of African and American aerosol emission removal, the range of precipitation changes is within 5-7%; however, there is a net increase (~3%) in the domain averaged precipitation for the experiment of Asian carbonaceous aerosol emission removal.

3.6 Potential Mechanism

In the previous sections, we have seen that as a response to NH carbonaceous emission removals from northern hemispheric hotspots, the maximum change to the global monsoon domain was observed in the NH. Interestingly, the global monsoon domain is largely dependent on summertime rainfall and atmospheric changes than the annual range itself (B. Wang et al., 2009). Hence the response of GM area and precipitation to spatially removing carbonaceous aerosol may be explained through the associated changes in the atmospheric state. In that context, we present the mean NH summertime vertical wind structure and the position of the Inter-Tropical Convergence Zone (ITCZ) for the CTRL and respective perturbation experiments in Fig. 7.

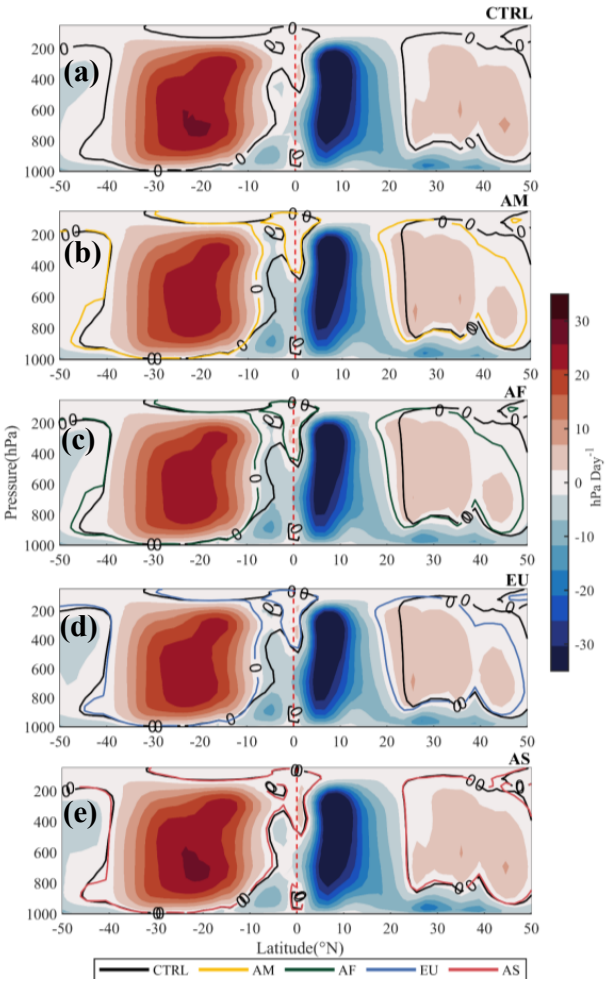

Figure 7. NH summer mean vertical pressure velocity showing the structure of ITCZ for (a) CTRL (b) AM, (c) AF (d) EU, and (e) AS simulations. The thick lines are the zero contour lines for respective simulations.

The position and strength of ITCZ can be distinguished by zonal mean vertical wind structure. ITCZ explains the area of maximum rainfall. During the NH summer monsoon months, the ITCZ position is over the land areas (negative vertical pressure velocity, blue color shading in Figure 7 a).

It is interesting to note that in the absence of carbonaceous aerosol emissions over the northern hemisphere (Figure 7 b-d), there is a southward shift of the zone of convergence except for the removal of Asian emission. Further, a slight increase in the subsidence takes place over the land around 20-30° N latitudes.

We further explain how the strength of ITCZ is changing as a response to the removal of remote carbonaceous aerosol emissions in Figure 8.

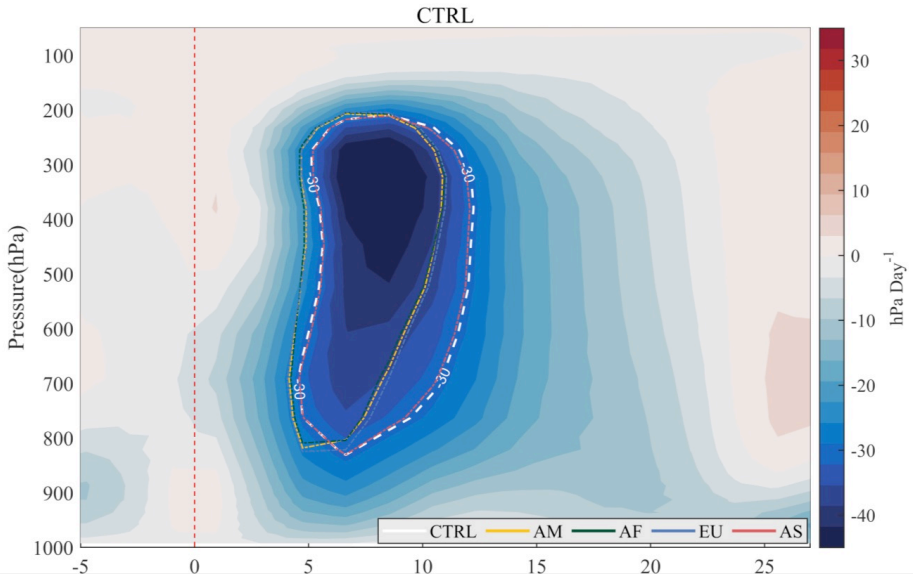

Figure 8. NH summertime mean position of ITCZ for CTRL. The coloured contour lines are the average of the top 50 percentile of maximum vertical wind speeds for respective simulations.

The shading shows the JJA mean position of ITCZ for CTRL simulation, whereas the contours are the average of the top 50 percentile vertical wind speeds for CTRL and perturbation experiments. It is clear from Fig. 8 that there is a shrink in the zones of maximum speeds. In addition, a southward shift in the contours of maximum speeds is observed, which is prominent in the middle and upper atmosphere for all the experiments except AS. Such changes can have substantial impacts to overall rainfall processes (Hari et al., 2020). We further illustrate the response of ITCZ to emission changes using a simple schematic in Figure 9.

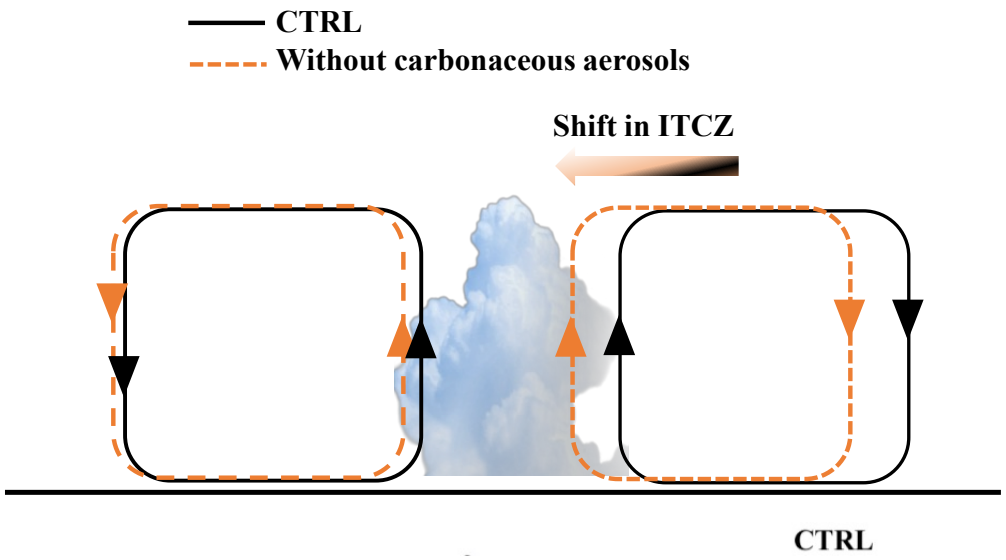

340

341 **Figure 9.** Schematic showing the response of ITCZ to northern hemispheric region-specific
342 removal of carbonaceous aerosol emissions.

343 **4.0 Discussion and Summary**

344 External forcing as well as internal feedbacks contribute to the variation of global
345 monsoon (GM) precipitation. Although the impact of internal variabilities under GHG-
346 induced global warming on GM is extensively studied, the role of external forcing like
347 aerosols is yet to be understood. From the results, it is evident that the total global monsoon
348 rainfall, as well as the areal extent, are influenced by the region-specific carbonaceous aerosol
349 emissions. These findings help in in adding more knowledge to the current understanding of
350 GM precipitation and their distribution under increasing GHG concentrations (Cherchi et al.,
351 2011). The aerosols-induced regional monsoon changes have been extensively investigated
352 in the past; however, understanding aerosol impacts on GM as a whole is relatively new.
353 Previous studies found the interlinks of GM to regionally varying volcanic emissions (Iles
354 and Hegerl, 2014; Liu et al., 2016a), while the roles of regional carbonaceous aerosols are
355 much less understood. Our results show that the North American and European carbonaceous
356 aerosols possess a larger impact on GM matrices than Asian aerosols (Figure 4-6). Similar
357 responses from sulfate emissions were reported in a recent study (Kasoar et al., 2018).

A few past studies using GCM reported a shift in the Intertropical Convergence Zone (ITCZ) due to the hemispheric asymmetry in aerosol forcing and hence a change in rainfall (Hwang et al., 2013; Krishnamohan et al., 2021). For example, Wang (Wang, 2004) reported an enhancement of the annual mean precipitation over India associated with a northward shift in ITCZ because of BC aerosols. A recent study (Modak and Bala, 2019) on the efficacy of BC aerosols found a northward shift of the ITCZ in response to global BC forcing. Because of this shift, they reported that the annual mean precipitation increases in the northern hemisphere tropics. It is important to note that these studies highlight the regional changes in precipitation (Modak and Bala, 2019; C. Wang et al., 2009; Wang, 2004) rather than the global monsoon as a whole. For the first time, we have shown the change in GM as a response to carbonaceous aerosol changes. In response to the spatially perturbed carbonaceous aerosols, we find a southward shift in the ITCZ as well as an alteration in its vertical structure (Figs. 7 and 8). The magnitude/strength of these changes reflected well in the changes in GM precipitation and area changes.

In recent decades, with the explosive economic development and rapid population growth in India and China, large amounts of BC aerosols are being emitted into the atmosphere and are known to have significant effects on the global and regional energy balance as well as climate (Bond et al., 2013; Li et al., 2016a; Ramanathan and Carmichael, 2008). In that aspect, the majority of previous studies focus on the Asian aerosol impacts on hydro-climatic implications. Our findings show that, although the change in AOD to carbonaceous emission removal over Asia is maximum globally and in NH (Figure 2), its impact on the global monsoon domain and precipitation is among the least. The sign of change in precipitation within the GM domain is opposite for Asian emission removal, to the emission removal from the other three regions. Again, here we quantify the impact of spatially varying remote

carbonaceous emissions on the ITCZ and thereby the GM characteristics rather than global aerosols as a whole shown by earlier studies (Krishnamohan et al., 2021; Modak and Bala, 2019). It is important to note that society may evolve and adopt policy measures gradually and hence regional and temporary emission reduction may continue to occur in the future. Hence, our results have interesting implications for emissions mitigation policies regionally when carbonaceous aerosol emissions are concerned. These findings also call for more detailed investigations into potential causes for such large differences in aerosol-induced changes in the global hydrological cycle.

One of the limitations of this modeling study is the use of a fixed SST setup (Bala et al., 2010b; Hansen, 2005). It is essential to note that carbonaceous aerosol emissions could have different impacts on regional and global monsoons based on their fast and slow adjustment contributions (Krishnamohan et al., 2021). The generalization of our findings is limited due to the use of a single model, as the computational efforts required for multiple sets of simulations are substantial. It is recommended for the modeling groups to investigate the response of similar regional emission perturbations in a coordinated manner using multi-model experiments. This would add statistical robustness to the climate implications of regional emission management policies. Additionally, this would complement the current emphasis on the simulation of historical and future climate scenarios, which does not separate the contributions of specific geopolitical regions.

Anthropogenic aerosol forcing is known to have spatial heterogeneity, mostly localized around industrialized regions of the world like Europe, North Africa, North America, East and South Asia. Emission reductions in each of these regions may impact the climate in different locations and may have diverse impacts on a regional and global scale. Using an

AGCM (CAM5) with explicit aerosol physics and radiative treatments, this study quantifies the response of global monsoon precipitation and spread (area) to regionally varying Northern Hemispheric carbonaceous aerosols. We summarize the findings as follows

1. Decreases in the global mean aerosol optical depth as a response to carbonaceous aerosol emission removal are -3.8 % for Asia followed by North America (-2.21 %), Africa (-1.8 %) and Europe (-1.16 %).
2. There is a southward shift in the NH monsoon domain when carbonaceous emissions are removed, which is maximum for EU followed by AF and AM, whereas least for AS.
3. The shift in the NH GM domain is in concert with the change in strength and position of the ITCZ.
4. Global monsoon domain and precipitation intensities are found to be influenced by carbonaceous aerosol removal with a contraction in the total GM area, and the magnitude of percentage departure is found to be the maximum for EU (~ -30%), followed by AM and AF (~ -25%).
5. The reduction in the area-averaged GM precipitation intensity is maximum for EU (~ -30 %) within the CTRL GM domain, which is halved for AF and AM cases (~ -15%). The impact of EU is ~4 folds higher in overall changes in GM precipitation when compared to AF and AM.
6. The response of GM precipitation and area are found to be near similar for AM and AF emission removal. The Asian carbonaceous aerosols have the least and opposite effects on GM area and precipitation.

Declaration of competing interests

The authors declare that they have no competing interests

Acknowledgements

AA is thankful to the ACOM-National Center for Atmospheric Research, Boulder, CO, USA. VV thanks ISRO for partial funding through its ARFINet program. K.L thanks partial funding through DST, Govt of India. HW acknowledges support by the U.S. Department of Energy (DOE), Office of Science, Office of Biological and Environmental Research, Earth and Environmental Systems Modeling program. The Pacific Northwest National Laboratory (PNNL) is operated for DOE by Battelle Memorial Institute under contract DE-AC05-76RLO1830.

Author contributions statement

A.A, K.L, H.W and VV conceived the idea. HW carried out the simulations, AA analyzed the model data and wrote the first draft of the paper. All the authors contributed equally to writing the manuscript.

Data and codes

The datasets and codes used in this study can be shared upon request to the corresponding author

References

Adler, R.F., Huffman, G.J., Chang, A., Ferraro, R., Xie, P.-P., Janowiak, J., Rudolf, B., Schneider, U., Curtis, S., Bolvin, D., Gruber, A., Susskind, J., Arkin, P., Nelkin, E., 2003. The Version-2 Global Precipitation Climatology Project (GPCP) Monthly Precipitation Analysis (1979 Present). JHyMe 4, 1147. https://doi.org/10.1175/1525-7541(2003)004

Bala, G., Caldeira, K., Nemani, R., 2010a. Fast versus slow response in climate change: implications for the global hydrological cycle. Clim. Dyn. 35, 423–434. https://doi.org/10.1007/s00382-009-0583-y

Bala, G., Caldeira, K., Nemani, R., 2010b. Fast versus slow response in climate change: Implications for the global hydrological cycle. Clim. Dyn. 35, 423–434. https://doi.org/10.1007/s00382-009-0583-y

Bollasina, M.A., Ming, Y., Ramaswamy, V., Schwarzkopf, M.D., Naik, V., 2014. Contribution of local and remote anthropogenic aerosols to the twentieth century weakening of the South Asian Monsoon. Geophys. Res. Lett. 41, 680–687. https://doi.org/10.1002/2013GL058183

Bond, T.C., Doherty, S.J., Fahey, D.W., Forster, P.M., Berntsen, T., Deangelo, B.J., Flanner, M.G., Ghan, S., Kärcher, B., Koch, D., Kinne, S., Kondo, Y., Quinn, P.K., Sarofim, M.C., Schultz, M.G., Schulz, M., Venkataraman, C., Zhang, H., Zhang, S., Bellouin, N., Guttikunda, S.K., Hopke, P.K., Jacobson, M.Z., Kaiser, J.W., Klimont, Z., Lohmann, U., Schwarz, J.P., Shindell, D., Storelvmo, T., Warren, S.G., Zender, C.S., 2013. Bounding the role of black carbon in the climate system: A scientific assessment. J. Geophys. Res. Atmos. 118, 5380–5552. https://doi.org/10.1002/jgrd.50171

Chakraborty, A., Nanjundiah, R.S., Srinivasan, J., 2013. Local and remote impacts of direct aerosol forcing on Asian monsoon. Int. J. Climatol. 2121, 2108–2121. https://doi.org/10.1002/joc.3826

Cherchi, A., Alessandri, A., Masina, S., Navarra, A., 2011. Effects of increased CO2 levels on monsoons. Clim. Dyn. 37, 83–101. https://doi.org/10.1007/S00382-010-0801-7

Ganguly, D., Rasch, P.J., Wang, H., Yoon, J.H., 2012. Climate response of the South Asian monsoon system to anthropogenic aerosols. J. Geophys. Res. Atmos. 117, D13209. https://doi.org/10.1029/2012jd017508

Gao, J., Yang, Y., Wang, H., Wang, P., Li, H., Li, M., Ren, L., Yue, X., Liao, H., 2022. Fast climate responses to emission reductions in aerosol and ozone precursors in China during 2013-2017. Atmos. Chem. Phys. 22, 7131–7142. https://doi.org/10.5194/ACP-22-7131-2022

Ghan, S.J., Liu, X., Easter, R.C., Zaveri, R., Rasch, P.J., Yoon, J.H., Eaton, B., 2012. Toward a minimal representation of aerosols in climate models: Comparative decomposition of aerosol direct, semidirect, and indirect radiative forcing. J. Clim. 25, 6461–6476. https://doi.org/10.1175/JCLI-D-11-00650.1

Guo, J., Yin, Y., 2015. Mineral dust impacts on regional precipitation and summer circulation in East Asia using a regional coupled climate system model. J. Geophys. Res. 120, 10378–10398. https://doi.org/10.1002/2015JD023096

Guo, L., Turner, A.G., Highwood, E.J., 2016. Local and remote impacts of aerosol species on indian summer monsoon rainfall in a GCM. J. Clim. 29, 6937–6955. https://doi.org/10.1175/JCLI-D-15-0728.1

Ha, K.J., Kim, B.H., Chung, E.S., Chan, J.C.L., Chang, C.P., 2020. Major factors of global and regional monsoon rainfall changes: natural versus anthropogenic forcing. Environ.

494 Res. Lett. 15. https://doi.org/10.1088/1748-9326/ab7767
495 Hansen, J., 2005. Efficacy of climate forcings. J. Geophys. Res. 110, D18104.
496 https://doi.org/10.1029/2005JD005776
497 Hari, V., Villarini, G., Karmakar, S., Wilcox, L.J., Collins, M., 2020. Northward
498 propagation of the inter tropical convergence zone and strengthening of Indian summer
499 monsoon rainfall. Geophys. Res. Lett. 47, e2020GL089823.
500 https://doi.org/10.1029/2020gl089823
501 Hsu, P.C., Li, T., Luo, J.J., Murakami, H., Kitoh, A., Zhao, M., 2012. Increase of global
502 monsoon area and precipitation under global warming: A robust signal? Geophys. Res.
503 Lett. 39, n/a-n/a. https://doi.org/10.1029/2012GL051037
504 Hsu, P.C., Li, T., Wang, B., 2011. Trends in global monsoon area and precipitation over the
505 past 30 years. Geophys. Res. Lett. 38, 1–5. https://doi.org/10.1029/2011GL046893
506 Hwang, Y.-T., Frierson, D.M.W., Kang, S.M., 2013. Anthropogenic sulfate aerosol and the
507 southward shift of tropical precipitation in the late 20th century.
508 https://doi.org/10.1002/grl.50502
509 Iles, C.E., Hegerl, G.C., 2014. The global precipitation response to volcanic eruptions in the
510 CMIP5 models. Environ. Res. Lett. 9, 104012. https://doi.org/10.1088/1748-
511 9326/9/10/104012
512 Kasoar, M., Shawki, D., Voulgarakis, A., 2018. Similar spatial patterns of global climate
513 response to aerosols from different regions. npj Clim. Atmos. Sci. 1, 12.
514 https://doi.org/10.1038/s41612-018-0022-z
515 Kay, J.E., Deser, C., Phillips, A., Mai, A., Hannay, C., Strand, G., Arblaster, J.M., Bates,
516 S.C., Danabasoglu, G., Edwards, J., Holland, M., Kushner, P., Lamarque, J.F.,
517 Lawrence, D., Lindsay, K., Middleton, A., Munoz, E., Neale, R., Oleson, K., Polvani,

L., Vertenstein, M., 2015. The community earth system model (CESM) large ensemble project : A community resource for studying climate change in the presence of internal climate variability. Bull. Am. Meteorol. Soc. 96, 1333–1349. https://doi.org/10.1175/BAMS-D-13-00255.1

Kitoh, A., Endo, H., Krishna Kumar, K., Cavalcanti, I.F.A., Goswami, P., Zhou, T., 2013. Monsoons in a changing world: A regional perspective in a global context. J. Geophys. Res. Atmos. 118, 3053–3065. https://doi.org/10.1002/jgrd.50258

Kripalani, R.H., Kulkarni, A., 2001. Monsoon rainfall variations and teleconnections over South and East Asia. Int. J. Climatol. 21, 603–616. https://doi.org/10.1002/JOC.625

Krishnamohan, K.S., Modak, A., Bala, G., 2021. Effects of local and remote black carbon aerosols on summer monsoon precipitation over India. Environ. Res. Commun. 3, 081003. https://doi.org/10.1088/2515-7620/AC18D1

Lamarque, J., Bond, T.C., Eyring, V., Granier, C., Heil, A., Klimont, Z., Lee, D., Liousse, C., Mieville, A., Insu, C., Latmos-ipsl, U.M.R., 2010. and Physics Historical (1850 – 2000) gridded anthropogenic and biomass burning emissions of reactive gases and aerosols : methodology and application 7017–7039. https://doi.org/10.5194/acp-10-7017-2010

Lau, K.M., Kim, M.K., Kim, K.M., 2006. Asian summer monsoon anomalies induced by aerosol direct forcing: the role of the Tibetan Plateau. Clim. Dyn. 26, 855–864. https://doi.org/10.1007/s00382-006-0114-z

Lau, W.K.M., 2016. The aerosol-monsoon climate system of Asia: A new paradigm. J. Meteorol. Res. 30, 1–11. https://doi.org/10.1007/s13351-015-5999-1

Lee, E.-J., Kyung-Ja, @bullet, @bullet, H., Jhun, J.-G., 2013. Interdecadal changes in interannual variability of the global monsoon precipitation and interrelationships

among its subcomponents. https://doi.org/10.1007/s00382-013-1762-4

Lee, J.Y., Wang, B., 2014. Future change of global monsoon in the CMIP5 42, 101–119.

Li, Z., Lau, W.K.-M., Ramanathan, V., Wu, G., Ding, Y., Manoj, M.G., Liu, J., Qian, Y., Li, J., Zhou, T., Fan, J., Rosenfeld, D., Ming, Y., Wang, Y., Huang, J., Wang, B., Xu, X., Lee, S.-S., Cribb, M., Zhang, F., Yang, X., Zhao, C., Takemura, T., Wang, K., Xia, X., Yin, Y., Zhang, H., Guo, J., Zhai, P.M., Sugimoto, N., Babu, S.S., Brasseur, G.P., 2016a. Aerosol and monsoon climate interactions over Asia. Rev. Geophys. 119–161. https://doi.org/10.1002/2015RG000500

Li, Z., Lau, W.K.M., Ramanathan, V., Wu, G., Ding, Y., Manoj, M.G., Liu, J., Qian, Y., Li, J., Zhou, T., Fan, J., Rosenfeld, D., Ming, Y., Wang, Y., Huang, J., Wang, B., Xu, X., Lee, S.S., Cribb, M., Zhang, F., Yang, X., Zhao, C., Takemura, T., Wang, K., Xia, X., Yin, Y., Zhang, H., Guo, J., Zhai, P.M., Sugimoto, N., Babu, S.S., Brasseur, G.P., 2016b. Aerosol and monsoon climate interactions over Asia. Rev. Geophys. 54, 866–929. https://doi.org/10.1002/2015rg000500

Liu, C., Yang, Y., Wang, H., Ren, L., Wei, J., Wang, P., Liao, H., 2023. Influence of Spatial Dipole Pattern in Asian Aerosol Changes on East Asian Summer Monsoon. J. Clim. 36, 1575–1585. https://doi.org/10.1175/JCLI-D-22-0335.1

Liu, F., Chai, J., Wang, B., Liu, J., Zhang, X., Wang, Z., 2016a. Global monsoon precipitation responses to large volcanic eruptions. Nat. Publ. Gr. https://doi.org/10.1038/srep24331

Liu, F., Chai, J., Wang, B., Liu, J., Zhang, X., Wang, Z., 2016b. Global monsoon precipitation responses to large volcanic eruptions. Sci. Rep. 6, 24331. https://doi.org/10.1038/srep24331

Liu, J., Wang, B., Ding, Q., Kuang, X., Soon, W., Zorita, E., 2009. Centennial Variations of

566 the Global Monsoon Precipitation in the Last Millennium: Results from ECHO-G
567 Model. J. Clim. 22, 2356–2371. https://doi.org/10.1175/2008JCLI2353.1
568 Liu, X., Easter, R.C., Ghan, S.J., Zaveri, R., Rasch, P., Shi, X., Lamarque, J.F., Gettelman,
569 A., Morrison, H., Vitt, F., Conley, A., Park, S., Neale, R., Hannay, C., Ekman, A.M.L.,
570 Hess, P., Mahowald, N., Collins, W., Iacono, M.J., Bretherton, C.S., Flanner, M.G.,
571 Mitchell, D., 2012. Toward a minimal representation of aerosols in climate models:
572 Description and evaluation in the Community Atmosphere Model CAM5. Geosci.
573 Model Dev. 5, 709–739. https://doi.org/10.5194/gmd-5-709-2012
574 Lou, S., Yang, Y., Wang, H., Smith, S.J., Qian, Y., Rasch, P.J., 2019. Black Carbon
575 Amplifies Haze Over the North China Plain by Weakening the East Asian Winter
576 Monsoon. Geophys. Res. Lett. 46, 452–460. https://doi.org/10.1029/2018GL080941
577 Ma, P.L., Rasch, P.J., Wang, H., Zhang, K., Easter, R.C., Tilmes, S., Fast, J.D., Liu, X.,
578 Yoon, J.H., Lamarque, J.F., 2013. The role of circulation features on black carbon
579 transport into the Arctic in the Community Atmosphere Model version 5 (CAM5). J.
580 Geophys. Res. Atmos. 118, 4657–4669. https://doi.org/10.1002/jgrd.50411
581 Man, W., Zuo, M., Zhou, T., Fasullo, J.T., Bethke, I., Chen, X., Zou, L., Wu, B., 2021.
582 Potential Influences of Volcanic Eruptions on Future Global Land Monsoon
583 Precipitation Changes. Earth's Futur. 9. https://doi.org/10.1029/2020EF001803
584 Meehl, G.A., Arblaster, J.M., Collins, W.D., 2008. Effects of black carbon aerosols on the
585 Indian monsoon. J. Clim. 21, 2869–2882. https://doi.org/10.1175/2007JCLI1777.1
586 Meehl, G.A., Covey, C., Delworth, T., Latif, M., McAvaney, B., Mitchell, J.F.B., Stouffer,
587 R.J., Taylor, K.E., 2007. The WCRP CMIP3 multimodel dataset: A new era in climatic
588 change research. Bull. Am. Meteorol. Soc. 88, 1383–1394.
589 https://doi.org/10.1175/BAMS-88-9-1383

590 Menon, S., 2002. Climate Effects of Black Carbon Aerosols in China and India. Science
591 (80-.). 297, 2250–2253. https://doi.org/10.1126/science.1075159
592 Modak, A., Bala, G., 2019. Efficacy of black carbon aerosols: the role of shortwave cloud
593 feedback. Environ. Res. Lett. 14, 084029. https://doi.org/10.1088/1748-9326/ab21e7
594 Myhre, G., Forster, P.M., Samset, B.H., Hodnebrog, Sillmann, J., Aalbergsjø, S.G.,
595 Andrews, T., Boucher, O., Faluvegi, G., Fläschner, D., Iversen, T., Kasoar, M., Kharin,
596 V., Kirkevag, A., Lamarque, J.F., Olivié, D., Richardson, T.B., Shindell, D., Shine,
597 K.P., Stjern, C.W., Takemura, T., Voulgarakis, A., Zwiers, F., 2017. PDRMIP: A
598 precipitation driver and response model intercomparison project-protocol and
599 preliminary results. Bull. Am. Meteorol. Soc. 98, 1185–1198.
600 https://doi.org/10.1175/BAMS-D-16-0019.1
601 Ramanathan, V., Carmichael, G., 2008. Global and regional climate changes due to black
602 carbon. Nat. Geosci. https://doi.org/10.1038/ngeo156
603 Ramanathan, V., Chung, C., Kim, D., Bettge, T., Buja, L., Kiehl, J.T., Washington, W.M.,
604 Fu, Q., Sikka, D.R., Wild, M., 2005a. Atmospheric brown clouds: Impacts on South
605 Asian climate and hydrological cycle. Proc. Natl. Acad. Sci. 102, 5326–5333.
606 https://doi.org/10.1073/pnas.0500656102
607 Ramanathan, V., Chung, C., Kim, D., Bettge, T., Buja, L., Kiehl, J.T., Washington, W.M.,
608 Fu, Q., Sikka, D.R., Wild, M., 2005b. Atmospheric brown clouds: Impacts on South
609 Asian climate and hydrological cycle. Proc. Natl. Acad. Sci. U. S. A. 102, 5326–5333.
610 https://doi.org/10.1073/pnas.0500656102
611 Ramesh, K. V., Goswami, P., 2007. Reduction in temporal and spatial extent of the Indian
612 summer monsoon. Geophys. Res. Lett. 34. https://doi.org/10.1029/2007GL031613
613 Rotstayn, L.D., Cai, W., Dix, M.R., Farquhar, G.D., Feng, Y., Ginoux, P., Herzog, M., Ito,

614 A., Penner, J.E., Roderick, M.L., Wang, M., 2007. Have Australian rainfall and
615 cloudiness increased due to the remote effects of Asian anthropogenic aerosols? J.
616 Geophys. Res. Atmos. 112, 1–28. https://doi.org/10.1029/2006JD007712
617 Samset, B.H., Sand, M., Smith, C.J., Bauer, S.E., Forster, P.M., Fuglestvedt, J.S., Osprey,
618 S., Schleussner, C.F., 2018. Climate Impacts From a Removal of Anthropogenic
619 Aerosol Emissions. Geophys. Res. Lett. 45, 1020–1029.
620 https://doi.org/10.1002/2017GL076079
621 Sanap, S.D., Ayantika, D.C., Pandithurai, G., Niranjan, K., 2014. Assessment of the aerosol
622 distribution over Indian subcontinent in CMIP5 models. Atmos. Environ. 87, 123–137.
623 https://doi.org/10.1016/j.atmosenv.2014.01.017
624 Sanap, S.D., Pandithurai, G., 2015. The effect of absorbing aerosols on Indian monsoon
625 circulation and rainfall: A review. Atmos. Res.
626 https://doi.org/10.1016/j.atmosres.2015.06.002
627 Schreck, C.J., Semazzi, F.H.M., 2004. Variability of the recent climate of eastern Africa.
628 Int. J. Climatol. 24, 681–701. https://doi.org/10.1002/JOC.1019
629 Shawki, D., Voulgarakis, A., 2018. The South Asian Monsoon Response to Remote
630 Aerosols : Global and Regional Mechanisms 585–601.
631 https://doi.org/10.1029/2018JD028623
632 Shawki, D., Voulgarakis, A., Chakraborty, A., Kasoar, M., Srinivasan, J., 2018. The South
633 Asian Monsoon Response to Remote Aerosols: Global and Regional Mechanisms. J.
634 Geophys. Res. Atmos. 123, 11,585-11,601. https://doi.org/10.1029/2018JD028623
635 Stocker, T.F., Qin, D., Plattner, G.K., Tignor, M.M.B., Allen, S.K., Boschung, J., Nauels,
636 A., Xia, Y., Bex, V., Midgley, P.M., 2013. Climate change 2013 the physical science
637 basis: Working Group I contribution to the fifth assessment report of the

638 intergovernmental panel on climate change, Climate Change 2013 the Physical Science
639 Basis: Working Group I Contribution to the Fifth Assessment Report of the
640 Intergovernmental Panel on Climate Change. Cambridge University Press.
641 https://doi.org/10.1017/CBO9781107415324
642 Trenberth, K.E., Stepaniak, D.P., Caron, J.M., 2000. The global monsoon as seen through
643 the divergent atmospheric circulation. J. Clim. 13, 3969–3993.
644 https://doi.org/10.1175/1520-0442(2000)013<3969:TGMAST>2.0.CO;2
645 Turner, A.G., Annamalai, H., 2012. Climate change and the South Asian summer monsoon.
646 Nat. Clim. Chang. 2, 587–595. https://doi.org/10.1038/NCLIMATE1495
647 Vinoj, V., Rasch, P.J., Wang, H., Yoon, J.H., Ma, P.L., Landu, K., Singh, B., 2014. Short-
648 term modulation of Indian summer monsoon rainfall by West Asian dust. Nat. Geosci.
649 7, 308–313. https://doi.org/10.1038/ngeo2107
650 Wang, B., 2006. The Asian monsoon. Springer.
651 Wang, B., Ding, Q., 2008. Global monsoon: Dominant mode of annual variation in the
652 tropics. Dynam Atmos Ocean. 44, 165–183.
653 https://doi.org/10.1016/j.dynatmoce.2007.05.002
654 Wang, B., Ding, Q., 2006. Changes in global monsoon precipitation over the past 56 years.
655 Geophys. Res. Lett. 33. https://doi.org/10.1029/2005GL025347
656 Wang, B., Liu, J., Kim, H.J., Webster, P.J., Yim, S.Y., 2012. Recent change of the global
657 monsoon precipitation (1979-2008). Clim. Dyn. 39, 1123–1135.
658 https://doi.org/10.1007/S00382-011-1266-Z
659 Wang, B., Liu, J., Yang, J., Zhou, T., Wu, Z., 2009. Distinct principal modes of early and
660 late summer rainfall anomalies in East Asia. J. Clim. 22, 3864–3875.
661 https://doi.org/10.1175/2009JCLI2850.1

662 Wang, C., 2004. A modeling study on the climate impacts of black carbon aerosols. J.
663 Geophys. Res. D Atmos. 109, D03106. https://doi.org/10.1029/2003jd004084
664 Wang, C., Kim, D., Ekman, A.M.L., Barth, M.C., Rasch, P.J., 2009. Impact of
665 anthropogenic aerosols on Indian summer monsoon. Geophys. Res. Lett. 36, L21704.
666 https://doi.org/10.1029/2009gl040114
667 Wang, H., Easter, R.C., Rasch, P.J., Wang, M., Liu, X., Ghan, S.J., Qian, Y., Yoon, J.-H.,
668 Ma, P.-L., Vinoj, V., 2013. Sensitivity of remote aerosol distributions to representation
669 of cloud–aerosol interactions in a global climate model. Geosci. Model Dev. 6, 765–
670 782. https://doi.org/10.5194/gmd-6-765-2013
671 Webster, P.J., Magana, V.O., Palmer, T.N., Shukla, J., Tomas, R.A., Yanai, M., Yasunari,
672 T., 1998. Monsoons: Processes, predictability, and the prospects for prediction. J.
673 Geophys. Res. 103, 451–14510.
674 Xie, X., Myhre, G., Liu, X., Li, X., Shi, Z., Wang, H., Kirkevåg, A., Lamarque, J.F.,
675 Shindell, D., Takemura, T., Liu, Y., 2020. Distinct responses of Asian summer
676 monsoon to black carbon aerosols and greenhouse gases. Atmos. Chem. Phys. 20,
677 11823–11839. https://doi.org/10.5194/acp-20-11823-2020
678 Yang, Y., Smith, S.J., Wang, H., Mills, C.M., Rasch, P.J., 2019. Variability, timescales, and
679 nonlinearity in climate responses to black carbon emissions. Atmos. Chem. Phys. 19,
680 2405–2420. https://doi.org/10.5194/acp-19-2405-2019
681 Yang, Y., Wang, H., Smith, S.J., Easter, R., Ma, P.L., Qian, Y., Yu, H., Li, C., Rasch, P.J.,
682 2017. Global source attribution of sulfate concentration and direct and indirect
683 radiative forcing. Atmos. Chem. Phys. 17, 8903–8922. https://doi.org/10.5194/acp-17-
684 8903-2017
685 Yu, R., Wang, B., Zhou, T., 2004. Tropospheric cooling and summer monsoon weakening

686 trend over East Asia. Geophys. Res. Lett. 31, 1–4.
687 https://doi.org/10.1029/2004GL021270
688 Zhou, P., Yang, X. Lou, Wang, X.G., Hu, B., Zhang, L., Zhang, W., Si, H.R., Zhu, Y., Li,
689 B., Huang, C.L., Chen, H.D., Chen, J., Luo, Y., Guo, H., Jiang, R. Di, Liu, M.Q., Chen,
690 Y., Shen, X.R., Wang, X., Zheng, X.S., Zhao, K., Chen, Q.J., Deng, F., Liu, L.L., Yan,
691 B., Zhan, F.X., Wang, Y.Y., Xiao, G.F., Shi, Z.L., 2020. A pneumonia outbreak
692 associated with a new coronavirus of probable bat origin. Nature 579, 270–273.
693 https://doi.org/10.1038/S41586-020-2012-7
694 Zhou, T., Zhang, L., Li, H., 2008. Changes in global land monsoon area and total rainfall
695 accumulation over the last half century. Geophys. Res. Lett. 35.
696 https://doi.org/10.1029/2008GL034881
697

Supplementary Section

Supplementary Table 1: Model configuration

Name	CAM5 (AGCM)
Spatial Resolution	2.5 x 1.9 degrees
Levels	30
Integration time step	30 minutes
Dynamic core	Finite Volume
Land	CLM4
Ocean/ice	Prescribed SST and sea ice concentrations
Aerosols	IPCC AR5
Radiations	RRTMG
Aerosol	3 modes (MAM3)
Aerosol direct and indirect effects (on warm and mixed-phase cirrus clouds) were included.	